Nanoscale

Cite this: *Nanoscale*, 2012, **4**, 461

www.rsc.org/nanoscale

PAPER

Atomically thin layers of MoS_2 *via* a two step thermal evaporation–exfoliation method†

Sivacarendran Balendhran,*[a] Jian Zhen Ou,[a] Madhu Bhaskaran,[a] Sharath Sriram,[a] Samuel Ippolito,[b] Zoran Vasic,[c] Eugene Kats,[d] Suresh Bhargava,[b] Serge Zhuiykov[d] and Kourosh Kalantar-zadeh*[a]

Received 13th July 2011, Accepted 9th October 2011
DOI: 10.1039/c1nr10803d

Two dimensional molybdenum disulfide (MoS_2) has recently become of interest to semiconductor and optic industries. However, the current methods for its synthesis require harsh environments that are not compatible with standard fabrication processes. We report on a facile synthesis method of layered MoS_2 using a thermal evaporation technique, which requires modest conditions. In this process, a mixture of MoS_2 and molybdenum dioxide (MoO_2) is produced by evaporating sulfur powder and molybdenum trioxide (MoO_3) nano-particles simultaneously. Further annealing in a sulfur-rich environment transforms majority of the excess MoO_2 into layered MoS_2. The deposited MoS_2 is then mechanically exfoliated into minimum resolvable atomically thin layers, which are characterized using micro-Raman spectroscopy and atomic force microscopy. Furthermore Raman spectroscopy is employed to determine the effect of electrochemical lithium ion exposure on atomically thin layers of MoS_2.

Introduction

Since the breakthrough of graphene synthesis,[1] the physics of two dimensional (2D) materials has received increasing attention. Although graphene demonstrates excellent properties as a 2D conductive material, it is not the most viable in the realm of semiconductor physics as it does not possess a natural band gap. The presence of a band gap allows the material to switch on and off, which is a crucial property in electronic devices. It has been reported that a tunable band gap can be introduced in bi-layer graphene using a perpendicular electrical field,[2] along with reports of several other methods such as shaping graphene sheets into nano-ribbon forms.[3] Notwithstanding such reports, the band gap is in the order of a few hundred meV. Additionally, the processes for introducing a band gap in graphene are generally complex, resulting in crystallographic damage to the material and loss in desirable electrical properties such as electron mobility.[4] Hence, layered transition metal oxides and sulfides (such as MoO_3, WO_3, and MoS_2) are promising and suitable candidates as 2D semiconducting materials due to their natural band gap.

In the recent years, the synthesis of 2D materials based on MoO_3,[5] WO_3,[6] and MoS_2[7,8] using simple mechanical exfoliation has generated significant interest. Of these, MoS_2 is a more favorable material compared to transition metal oxides, since it has a relatively small band gap of 1.29 eV and 1.90 eV for the bulk material and single layers, respectively.[9] In addition MoS_2 is not fully saturated in sulfur, compared to MoO_3 and WO_3 which are in their maximum oxidation states.[10] Due to these characteristics, MoS_2 presents a wide range of applications such as mass-sensitive liquid pollutant sensors,[10] selective gas sensors,[11] catalysts,[12] hydrogen storage,[13] nano-lubricants,[14–16] lithium ion battery anodes[16,17] and biomedical applications.[18]

The basic unit of MoS_2 is composed of a molybdenum atom coordinated with six sulfur atoms (Fig. 1). It is organized in two layers of sulfur atoms forming a sandwich structure, with a layer of molybdenum atoms in the middle. Each sulfur atom is coordinated with three molybdenum atoms within a single 2D layer of MoS_2. The bulk material is formed of these 2D layers held together by van der Waals forces.[19] It has been demonstrated that these van der Waals forces are weak enough to let the material split into minimum resolvable atomic layers through mechanical[7,9] and liquid[20,21] exfoliation techniques. These atomically thin layers of MoS_2 display enhanced electrical and optical properties due to the quantum confinement effect.[7] Although the first measurements of carrier mobility in atomically thin layers of MoS_2 resulted in the observation of relatively small values in the range of 0.5–3.0 $cm^2\ V^{-1}\ s^{-1}$,[22] Radisavljevic *et al.* have recently demonstrated the dramatic increase in electron mobility through a top gate approach in a field effect measurement. In this seminal work, by depositing a high dielectric material such as hafnium

---

[a] *School of Electrical and Computer Engineering, RMIT University, Melbourne, VIC, Australia. E-mail: shiva.balendhran@rmit.edu.au; kourosh.kalantar@rmit.edu.au*
[b] *School of Applied Sciences, RMIT University, Melbourne, VIC, Australia*
[c] *Melbourne Centre for Nano Fabrication, Clayton, VIC, Australia*
[d] *Materials Science and Engineering Division, CSIRO, Highett, VIC, Australia*

† Electronic supplementary information (ESI) available: Further AFM scans and a discussion on the reaction mechanisms are included. See DOI: 10.1039/c1nr10803d

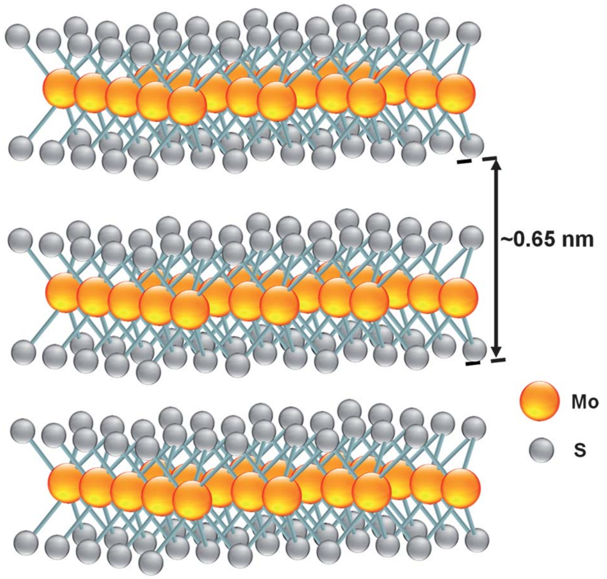

Fig. 1 Visualization of the atomic structure of layered hexagonal MoS_2.

dioxide (HfO_2) on atomically thin MoS_2, a mobility of ~217 cm^2 V^{-1} s^{-1} has been reported.[7] Such an increase in carrier mobility is of fundamental importance in the electronics industry for the development of high gain and fast switching transistors. Splendiani *et al.* have also reported the transformation of MoS_2 band structure from indirect to direct band gap at 2D levels,[8] while demonstrating significant photoluminescence owing to this change in the band structure.[8,9] Such a direct band gap is also of elemental significance as it allows engineering novel optical behaviors and holds promise for new nanophotonic applications.

The development of 2D materials is generally a two-step process: the synthesis of the layered bulk material followed by the exfoliation process.[1,6] Although there is a wide range of controlled methods of synthesis available to produce different morphologies of MoS_2 such as hydrothermal,[23] solvothermal,[24] chemical transport reaction,[25] and high pressure-arc discharge,[26] synthesis of layered MoS_2 is a topic that is yet to be widely explored. A few known methods of layered MoS_2 synthesis are thermal decomposition of ammonium thiomolybdate precursors[12] and chemical reactions between sulfur and molybdenum based compounds.[10,27] These methods consist of highly controlled parameters (pressure, temperature, *etc.*), and also require complex chemical experimental apparatus (three zone furnace, autoclave setups, *etc.*).[25,27,28] Some of these methods involve hazardous materials such as hydrogen sulfide (H_2S) and carbon disulfide (CS_2)[12,27] and are also conducted over a long period of time[27] yield them unfavorable for applications in electronic and optical device fabrication industries.

One of the less explored methods for the fabrication of layered MoS_2 is thermal evaporation. Thermal evaporation in a horizontal furnace involves annealing commercially available materials containing molybdenum and sulfur at the required temperature in gaseous carriers.[29] Although this is a simple, fast and controllable process, thermal evaporation of commercial MoS_2 powder has so far not been considered since the evaporation temperature of MoS_2 is prohibitively high (1375 °C).

In this work, we report a simple method for synthesis of layered MoS_2 through thermal evaporation of MoO_3 nanopowder along with excess sulfur, overcoming the direct evaporation barrier with MoS_2. Additionally this approach does not produce hazardous gasses and also does not require complex experimental setups. The synthesis of MoS_2 by the co-evaporation process was carried out at various annealing temperatures and for different durations. The resulting thin films are then characterized using scanning electron microscopy (SEM), micro-Raman spectroscopy, and X-ray diffraction (XRD) techniques. Mechanical exfoliation is conducted on the acquired samples and the flakes are analyzed using Raman spectroscopy and atomic force microscopy (AFM). Lithium ion exposure studies of such layers are presented to demonstrate their unique properties in comparison to their thicker counterparts.

Experimental

The thermal evaporation technique was applied in a horizontal furnace incorporating a quartz tube (Fig. 2). MoO_3 powder

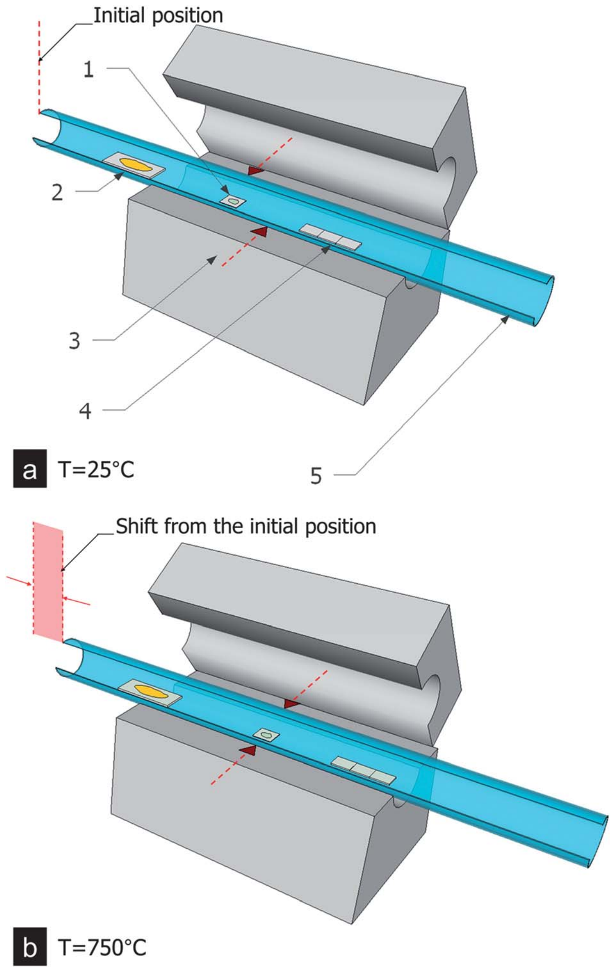

Fig. 2 Experimental setup: (a) initially at room temperature, the centre of the tube is offset from the centre of the furnace and in (b) at 750 °C, the tube is pushed inside the furnace aligning the centre of the tube with the centre of the furnace. Legend: (1) MoO_3 nanopowder, (2) sulfur powder, (3) horizontal furnace, (4) quartz substrates for deposition and (5) quartz tube.

weighing 50 mg (99% purity, China Rare Material Company) was placed on a quartz substrate, which was then positioned in the center of the tube. Sulfur powder (99% purity, Sigma-Aldrich) was placed upstream relative to the gas flow direction, 20 cm from the MoO_3 powder. Quartz substrates were placed along the downstream side for the MoS_2 deposition.

The deposition process was conducted by evaporating sulfur powder and MoO_3 nano-particles simultaneously in an argon environment at a flow rate of 200 sccm. Further annealing was conducted in a sulfur rich environment to enhance the presence of MoS_2. Initially, the center of the quartz tube was offset from the center of the furnace and was heated at a rate of 20 °C min^{-1} (Fig. 2a). As soon as the center of the furnace reached 750 °C the quartz tube was pushed in (Fig. 2b), placing the center of the tube at the center of the furnace. This procedure allows the MoO_3 and the sulfur to evaporate at the same time. Afterwards, the setup was held at the set temperature for the experimented annealing duration. The thermal evaporation process was carried out at different temperatures and durations in order to determine the optimal experimental conditions for layered MoS_2 deposition. Three annealing conditions are presented in this work: (a) 775 °C for 60 min, (b) 830 °C for 60 min and (c) 830 °C for 180 min. At the end of the process, the temperature was ramped down at 20 °C min^{-1} until room temperature was reached.

The obtained thin films were characterized using scanning electron microscopy, X-ray diffraction and Raman spectroscopy. SEM micrographs were acquired using a FEI Nova Nanoscope and the XRD diffractograms were obtained using a Bruker D8 micro-diffractometer equipped with a general area detector diffraction system (GADDS). Data were collected at room temperature using a copper source with a potential of 40 kV and a current of 40 mA. The Raman measurements were performed over an accumulation time of 10 s for 3 accumulations using an Ocean Optics QE6500 spectrometer equipped with a 532 nm, 40 mW laser source.

In order to obtain thin layered MoS_2, adhesive tape was used on the deposited film to mechanically exfoliate the flakes[5,6] and transfer them onto silica on silicon (SiO_2/Si) substrates. Raman measurements on the exfoliated flakes were conducted over an accumulation time of 120 s for 2 accumulations using a Jobin Yvon Horiba TRIAX 320 spectrometer equipped with a 532 nm, 0.7 mW laser source.

Atomic force microscopy was carried out on a Veeco Dimension Icon scanning probe microscope. For electrochemical ion intercalation, saturated lithium chloride (LiCl) solution was prepared at room temperature. Mechanically exfoliated MoS_2 flakes were transferred onto a conductive substrate (tungsten 25 nm on SiO_2/Si substrates) and Raman spectra were acquired for selected flakes. Platinum (Pt) foil was utilized as the anode and the conductive substrate containing the flakes as the cathode. Both the anode and cathode were completely submerged into the LiCl solution. A voltage of 4 V DC, for a duration of 4 min, was applied, allowing enough time for the intercalation process. The flakes were then located and Raman spectra were acquired to determine the effect of Li^+ exposure.

Results and discussion

Micrographs of the deposited MoS_2 thin films reveal the effect of the temperature and annealing duration on surface morphology. Fig. 3a shows the film obtained by annealing at 775 °C for 60 min. The film does not have a well-defined structure. The magnified view of the surfaces and the blunt edges of these crystals indicates the possibility of rather amorphous growth achieved at lower temperatures. The increase in the temperature (830 °C) for the same annealing duration seems to have shifted the crystal growth towards layered structures. Fig. 3b illustrates these smooth surfaces and refined edges of the morphology acquired at 830 °C. Fig. 3c provides a view of the general surface morphology of the deposition achieved by further increasing the annealing duration to 180 min at 830 °C. The surface proves to be a collection of randomly stacked micro-platelets. These layered platelets seem to have average side lengths of a few micrometres. Well defined flakes with sharp edges and smooth layered surfaces have been produced, as shown in Fig. 3d. The thicknesses of these structures have been observed to be around 30 nm or less (Fig. 3e).

Raman spectroscopy was carried out to analyze the bond symmetry in the deposited thin films. In all three cases, Raman peaks corresponding to MoS_2 were observed (Fig. 4). The vibration of Mo–S bond (E_{2g}^1) along the base plane was observed at 381 cm^{-1} and vibration of sulfur along the vertical (A_{1g}) axis was observed at 406 cm^{-1}.[19,25] For the deposition at 775 °C for 60 min, broad MoS_2 peaks were observed (Fig. 4a). As the annealing temperature was increased to 830 °C for the same annealing duration, the spectra reveal better defined peaks

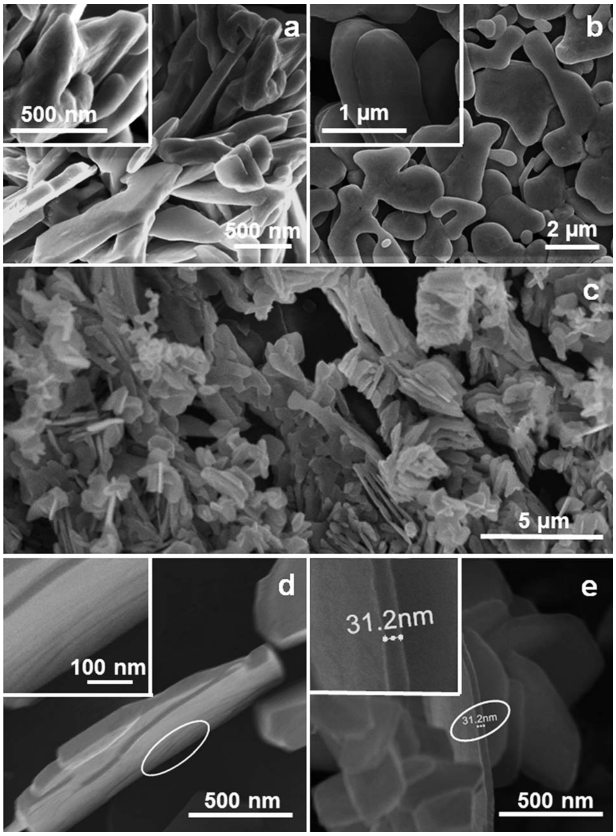

Fig. 3 Scanning electron micrographs of the MoS_2 deposition on quartz substrates obtained by thermal evaporation and annealed at: (a) 775 °C for 60 min, (b) 830 °C for 60 min, and (c–e) 830 °C for 180 min.

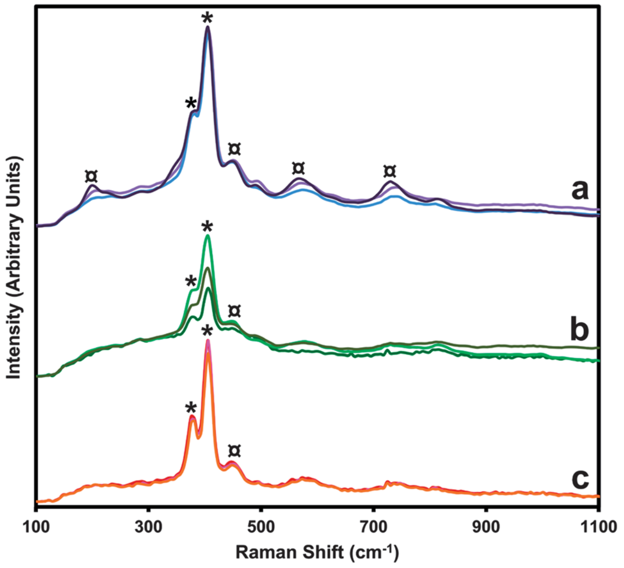

Fig. 4 Raman spectra of MoS_2 deposition on quartz substrates: (a) annealed at 775 °C for 60 min, (b) annealed at 830 °C for 60 min, and (c) annealed at 830 °C for 180 min (peaks correspond to [*] MoS_2 and [¤] MoO_2).

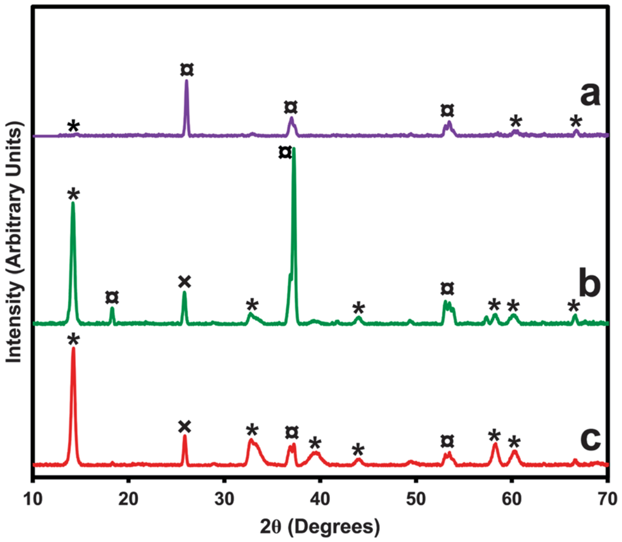

Fig. 5 XRD patterns of MoS_2 deposition on quartz substrates: (a) annealed at 775 °C for 60 min, (b) annealed at 830 °C for 60 min, and (c) annealed at 830 °C for 180 min (peaks correspond to [*] MoS_2, [¤] MoO_2 and [×] MoO_3). The results display the progress of MoS_2 formation from MoO_2 in correspondence with temperature and time.

(Fig. 4b) in comparison with the samples acquired at lower temperatures. By increasing the annealing duration from 60 min to 180 min, well-defined narrow peaks were observed at 830 °C (Fig. 4c). Also observed were weak peaks corresponding to MoO_2. Based on these observations, for temperatures less than 775 °C, the deposited film is nanocrystalline and as the temperature increases to 830 °C a more crystalline MoS_2 is obtained. As the annealing duration was further increased to 180 min, the observed narrow Raman peaks indicate the presence of highly ordered layered structures. Raman spectroscopy results concur with the surface morphologies observed in the SEM micrographs (Fig. 3).

XRD was used to study the crystal structure of the deposited thin films. The XRD pattern of the as-deposited samples annealed at 775 °C for 60 minutes (Fig. 5a) reflects the dominant peak at 2θ of 26.08° corresponding to the (011) plane of MoO_2 (ICDD Card no: 76-1807). Secondary peaks at 37.4°, 53.3°, and 53.6° corresponding to MoO_2 were also observed. Peaks corresponding to MoS_2 could be barely resolved. When the temperature increased to 830 °C however for smaller annealing duration, the dominant peak was observed at 37.4° corresponding to the (002) plane of MoO_2 (Fig. 5b). This time the peak reflecting the (002) plane of layered hexagonal MoS_2 at 14.4° (ICDD Card no: 77-1716) was also observed. The MoS_2 peaks appeared in intensities significantly larger than the deposition achieved in the lower temperature case. In addition, a peak corresponding to the (001) plane of MoO_2 was observed at 18.4° indicating better crystallinity in comparison with the film obtained at 775 °C. For the sample annealed at 830 °C for 180 min, the intensity of the (002) MoO_2 peak was significantly lower, with the (002) MoS_2 peak emerging as the dominant peak indicating the larger presence of ordered MoS_2 (Fig. 5c). This spectrum shows the dominant presence of well-stacked, highly crystalline 2H–MoS_2. The peaks at 32.7°, 33.5°, and 58.3° correspond to (100), (101), and (110) planes of 2H–MoS_2, respectively. In this case, intensities of all MoO_2 peaks have significantly reduced in contrast to the MoS_2 peaks, indicating that the film has dominantly transformed into MoS_2. Peaks corresponding to MoO_3 were observed in the case of the higher temperature process. We believe that at this temperature sulfur replaces oxygen in MoO_2 to form MoS_2. The released oxygen ions at higher temperatures along with the lack of gaseous sulfur contribute to the re-oxidation of a fraction of MoO_2 to MoO_3. Similar observation has been reported by Ressler *et al.* in a study of H_2 based reduction of MoO_3.[30] Further discussion can be found in the ESI†. Based on the collective observation, it is apparent that at lower synthesis temperatures, the concentration of MoS_2 in the films is significantly lower than MoO_2. At the increased temperatures of 830 °C, a combination of crystalline MoS_2 and MoO_2 deposition is obtained. With the increase of annealing duration at 830 °C, the presence of MoO_2 is significantly reduced and dominantly MoS_2 is achieved. From these experiments, it can be concluded that the reaction occurs in two phases: phase one involves sulfur vapor reducing MoO_3 to MoO_2 and in the second phase the excess sulfur reacts with MoO_2 and produces MoS_2. The process temperature and reaction duration determine the degree of conversion of the original MoO_3 powder into a thermally evaporated MoS_2 film.

Mechanical exfoliation was conducted on the samples evaporated at 830 °C and annealed for 180 min, which was dominantly MoS_2. Atomic force microscopy was used to determine the thickness and the presence of a layered structure in the exfoliated flakes. The thickness analysis through atomic force microscopy reveals flakes with typical thicknesses ranging from 5 to 50 nm. The atomic force microscopy results also concur that the exfoliated flakes are indeed layered (Fig. 6). Fig. 6a illustrates a random MoS_2 flake mainly consisting of four fundamental atomic layers. Cross-sectional profiling also shows that some

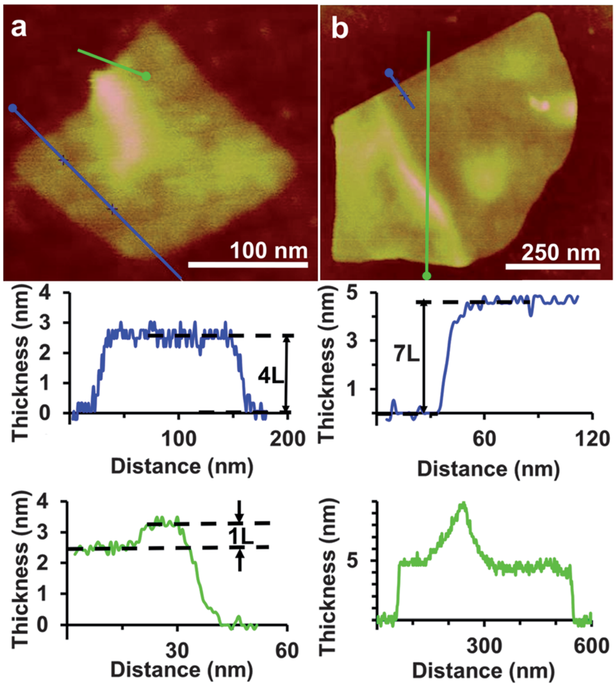

Fig. 6 AFM scans of two different MoS_2 flakes exfoliated on SiO_2/Si substrates and their corresponding cross-sectional thicknesses: (a) flake consisting of clearly resolved single step on its surface and (b) a large flake made of 7 layers showing a slightly folded structure.

parts of the flake consists of several more layers that are stacked on its surface. A step of ~0.65 nm can be clearly resolved in Fig. 6a, which corresponds to the fundamental thickness of a single atomic layer of MoS_2.[7] Additionally, a MoS_2 flake consisting of approximately seven layers can be seen in Fig. 6b. Interestingly, surface bulges and folds can be recognized in the image. This indicates that a few layers of MoS_2 can be flexible enough to be bent without breaking, similar to graphene sheets.[31] Additional cross-sectional AFM scans are available in the ESI†.

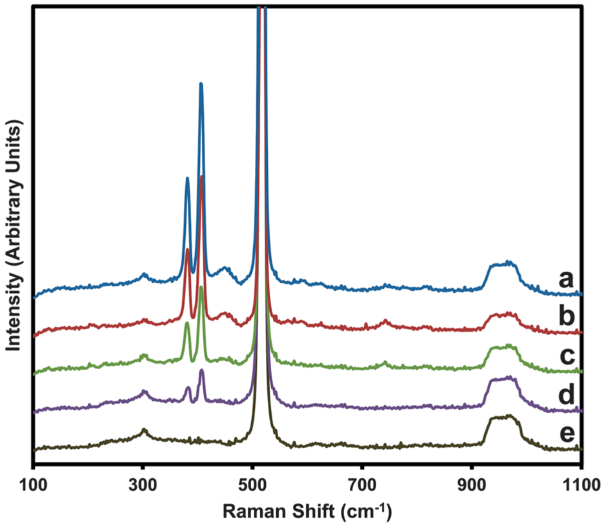

Fig. 7 Raman spectra of (a–d) exfoliated MoS_2 flakes with thickness reducing from (a) to (d) in a range of 50 nm to 5 nm and (e) background substrate SiO_2/Si.

Micro-Raman spectroscopy was employed for characterizing the exfoliated flakes as it has been proven to be an excellent tool for assessing 2D materials, which are obtained *via* the exfoliation method.[1,22] Raman spectra of randomly exfoliated flakes of different thicknesses were obtained in order to determine their composition. Spectra of the exfoliated flakes with thicknesses reducing from 50 to 5 nm are presented in Fig. 7a–d. The obtained spectra reveal vibration modes for the flakes identical to the as-deposited MoS_2 films with no MoO_2 contamination with reducing thickness. This suggests that the top surface of the synthesized films is dominantly MoS_2 and the observed MoO_2 contribution in the X-ray diffractograms is mainly from the bottom of the films. The strong peak at 521 cm^{-1} and the other weak features around 300 and 900–1000 cm^{-1} in the spectra correspond to the silica on the silicon substrate, and is verified by a background spectral measurement (Fig. 7e).

Raman spectroscopy was used to characterize the effect of lithium ion (Li^+) exposure for two exfoliated flakes of different thicknesses. Fig. 8 shows the Raman spectrum acquired before and after Li^+ exposure of two randomly targeted flakes. Lee *et al.* reported the shift of Raman peaks for $E_{2g}{}^1$ and A_{1g} at a level of

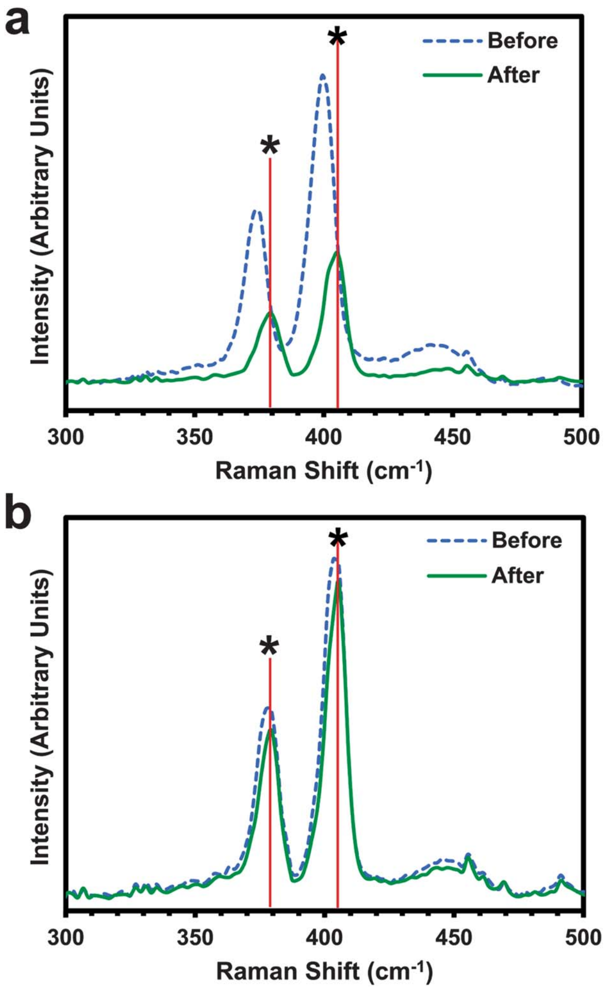

Fig. 8 Raman spectra acquired before and after Li^+ intercalation of two different MoS_2 flakes: (a) thickness ≈ 10 nm and (b) thickness > 20 nm. [*] represents the MoS_2 peak locations corresponding to the as-deposited thin films.

few atomic layers[32] in comparison with the bulk material. This can be observed in Fig. 8: the spectra for flakes in Fig. 8a (thickness ≈ 10 nm) and in Fig. 8b (thickness > 20 nm) both show a shift in E_{2g}^1 and A_{1g} modes before the intercalation with respect to the bulk material. For both flakes, after the Li^+ exposure the peak shift is observed to the right with respect to the initial Raman spectra before the exposure. The shift observed in the Raman spectra can be related to a strain introduced into these bonds, which is due to the interstitial occupation by Li^+.[33] However as observed, the shift is significantly larger for the thinner flake. This can be due to a better efficiency for the intercalation of the Li^+, when the number of layers is reduced. In addition, a significant reduction in the intensity of the Raman spectrum can also be observed for the thin flake. This is in agreement with the report by Julien *et al.*, who also observed similar reductions for bulk MoS_2,[33] which they ascribed to the mild Li^+ intercalation forming $Li_{0.1}MoS_2$. More detailed Raman spectroscopy based studies for Li^+ intercalation of thin layered MoS_2 are to be undertaken in future work.

Conclusion

We have demonstrated the successful synthesis of layered hexagonal MoS_2, through a simple method of thermal evaporation in a reduction environment. This method uses temperatures less than 830 °C which is much less than the temperature, which is required for the direct evaporation of MoS_2. By the application of the mechanical exfoliation technique on the layered MoS_2, we have obtained atomically thin layers of MoS_2 with the steps of ~0.65 nm corresponding to the fundamental thickness of the material. These atomically thin layers can be utilized in the fabrication of electronic devices of high carrier mobility to pave the way into the next generation of electronic devices.

Acknowledgements

MB and SS acknowledge the Australian Post-Doctoral Fellowships from the Australian Research Council through Discovery Projects DP1092717 and DP110100262, respectively. SS and KKZ acknowledge the Australian Research Council for equipment funding through the Linkage, Infrastructure, Equipment, and Facilities Grant LE100100215. The work was partially supported by the CSIRO Sensors and Sensor Networks Transformational Capability Platform and CSIRO Materials Science and Engineering Division—strategic co-investment SIP6 project "Nano Scale Sensor Networks".

Notes and references

1 K. S. Novoselov, A. K. Geim, S. V. Morozov, D. Jiang, Y. Zhang, S. V. Dubonos, I. V. Grigorieva and A. A. Firsov, *Science*, 2004, **306**, 666–669.
2 Y. Zhang, T.-T. Tang, C. Girit, Z. Hao, M. C. Martin, A. Zettl, M. F. Crommie, Y. R. Shen and F. Wang, *Nature*, 2009, **459**, 820–823.
3 M. Y. Han, B. Ozyilmaz, Y. B. Zhang and P. Kim, *Phys. Rev. Lett.*, 2007, **98**, 206805.
4 X. L. Li, X. R. Wang, L. Zhang, S. W. Lee and H. J. Dai, *Science*, 2008, **319**, 1229–1232.
5 K. Kalantar-zadeh, A. Vijayaraghavan, M. H. Ham, H. D. Zheng, M. Breedon and M. S. Strano, *Chem. Mater.*, 2010, **22**, 5660–5666.
6 K. Kalantar-zadeh, J. S. Tang, M. S. Wang, K. L. Wang, A. Shailos, K. Galatsis, R. Kojima, V. Strong, A. Lech, W. Wlodarski and R. B. Kaner, *Nanoscale*, 2010, **2**, 429–433.
7 B. Radisavljevic, A. Radenovic, J. Brivio, V. Giacometti and A. Kis, *Nat. Nanotechnol.*, 2011, **6**, 147–150.
8 A. Splendiani, L. Sun, Y. B. Zhang, T. S. Li, J. Kim, C. Y. Chim, G. Galli and F. Wang, *Nano Lett.*, 2010, **10**, 1271–1275.
9 K. F. Mak, C. Lee, J. Hone, J. Shan and T. F. Heinz, *Phys. Rev. Lett.*, 2010, **105**, 136805.
10 P. A. Lieberzeit, A. Aftal, A. Rehman and F. L. Dickert, *Sens. Actuators, B*, 2007, **127**, 132–136.
11 B. K. Miremadi, R. C. Singh, S. R. Morrison and K. Colbow, *Appl. Phys. A: Mater. Sci. Process.*, 1996, **63**, 271–275.
12 H. Farag, A. N. A. El-Hendawy, K. Sakanishi, M. Kishida and I. Mochida, *Appl. Catal., B*, 2009, **91**, 189–197.
13 J. Chen and F. Wu, *Appl. Phys. A: Mater. Sci. Process.*, 2004, **78**, 989–994.
14 V. N. Bakunin, A. Y. Suslov, G. N. Kuzmina, O. P. Parenago and A. V. Topchiev, *J. Nanopart. Res.*, 2004, **6**, 273–284.
15 C. Lee, Q. Y. Li, W. Kalb, X. Z. Liu, H. Berger, R. W. Carpick and J. Hone, *Science*, 2010, **328**, 76–80.
16 J. Xiao, D. W. Choi, L. Cosimbescu, P. Koech, J. Liu and J. P. Lemmon, *Chem. Mater.*, 2010, **22**, 4522–4524.
17 K. Chang, W. Chen, L. Ma, H. Li, H. Li, F. Huang, Z. Xu, Q. Zhang and J.-Y. Lee, *J. Mater. Chem.*, 2011, **21**, 6251–6257.
18 H. H. Wu, R. Yang, B. M. Song, Q. S. Han, J. Y. Li, Y. Zhang, Y. Fang, R. Tenne and C. Wang, *ACSNano*, 2011, **5**, 1276–1281.
19 T. J. Wieting and J. L. Verble, *Phys. Rev. B: Solid State*, 1971, **3**, 4286–4292.
20 A. S. Golub, D. P. Rupasov, N. D. Lenenko and Y. N. Novikov, *Russ. J. Inorg. Chem.*, 2010, **55**, 1166–1171.
21 J. N. Coleman, M. Lotya, A. O'Neill, S. D. Bergin, P. J. King, U. Khan, K. Young, A. Gaucher, S. De, R. J. Smith, I. V. Shvets, S. K. Arora, G. Stanton, H. Y. Kim, K. Lee, G. T. Kim, G. S. Duesberg, T. Hallam, J. J. Boland, J. J. Wang, J. F. Donegan, J. C. Grunlan, G. Moriarty, A. Shmeliov, R. J. Nicholls, J. M. Perkins, E. M. Grieveson, K. Theuwissen, D. W. McComb, P. D. Nellist and V. Nicolosi, *Science*, 2011, **331**, 568–571.
22 K. S. Novoselov, D. Jiang, F. Schedin, T. J. Booth, V. V. Khotkevich, S. V. Morozov and A. K. Geim, *Proc. Natl. Acad. Sci. U. S. A.*, 2005, **102**, 10451–10453.
23 Y. Tian, Y. He and Y. Zhu, *Chem. Lett.*, 2003, **32**, 768–769.
24 D. Duphil, S. Bastide and C. Levy-Clement, *J. Mater. Chem.*, 2002, **12**, 2430–2432.
25 M. Virsek, M. Krause, A. Kolitsch and M. Remskar, *Phys. Status Solidi B*, 2009, **246**, 2782–2785.
26 M. Chhowalla and G. A. J. Amaratunga, *Nature*, 2000, **407**, 164–167.
27 X. Y. Chen, X. Wang, Z. H. Wang, W. C. Yu and Y. T. Qian, *Mater. Chem. Phys.*, 2004, **87**, 327–331.
28 G. W. Li, C. S. Li, H. Tang, K. S. Cao, J. A. Chen, F. F. Wang and Y. Jin, *J. Alloys Compd.*, 2010, **501**, 275–281.
29 X. L. Li and Y. D. Li, *Chem.–Eur. J.*, 2003, **9**, 2726–2731.
30 T. Ressler, R. E. Jentoft, J. Wienold, M. M. Gunter and O. Timpe, *J. Phys. Chem. B*, 2000, **104**, 6360–6370.
31 X. Q. Zhang, S. H. Wan, J. B. Pu, L. P. Wang and X. Q. Liu, *J. Mater. Chem.*, 2011, **21**, 12251–12258.
32 C. Lee, H. Yan, L. E. Brus, T. F. Heinz, J. Hone and S. Ryu, *ACS Nano*, 2010, **4**, 2695–2700.
33 C. Julien, T. Sekine and M. Balkanski, *Solid State Ionics*, 1991, **48**, 225–229.